A Nonsymmetric Equatorial Inertial Instability

TIMOTHY J. DUNKERTON
Physical Dynamics, Inc., P.O. Box 3027, Bellevue, WA 98009

10 June 1982 and 1 November 1982

ABSTRACT

Inertial instabilities on the equatorial beta-plane may take the form of a zonally nonsymmetric disturbance while preserving their centrifugal character. Numerical experiments at finite zonal wavenumber suggest a preferred mode of instability with zonal wavenumber between the symmetric value and a short-wave cutoff in linear cross-equatorial shear. Zonal nonsymmetry results in a slight reduction of the marginally stable shear in the presence of second-order diffusion.

1. Introduction

The theory of hydrodynamic instability is fundamental to the atmospheric and oceanic sciences. As noted by Lindzen and Tung (1978), one may, for qualitative purposes, distinguish "shear instabilities" and "parcel instabilities" among those instabilities believed to be relevant to the atmosphere and ocean. The former instabilities may be interpretable in terms of wave overreflection, while the latter class of instabilities can be more simply described in terms of forces acting on individual fluid parcels. Familiar examples of shear instability are barotropic, baroclinic, and stratified shear instability. Relevant parcel instabilities are convective and inertial instability.

This distinction between shear and parcel instability may become somewhat unclear in certain cases, although the relationships between the two classes have hardly been explored at all. This may prove to be the case in the context of a specific problem to be reported in this note, *viz.* the instability of linear cross-equatorial shear. It will be noted that this particular shear is stable with respect to the overreflecting *barotropic* instabilities, as there is zero "curvature" of the mean flow, i.e., $\bar{u}_{yy} = 0$. However, as first noted by Dunkerton (1981), a linear *cross-equatorial* shear is inertially, or centrifugally, unstable in the inviscid case. (In this context, *centrifugally stable* refers to the nonvanishing mean vorticity. Our interest is in angular momentum instabilities not dependent on finite Richardson numbers for their existence.) The unstable eigensolutions, which are analytically described in terms of Hermite functions shifted off the equator, strongly resemble the familiar inertial "rolls" between differentially rotating concentric cylinders. However, in the equatorial case trapping is provided by the beta-effect, as is true of equatorial waves in general, instead of cylindrical sidewalls. Large amplitudes exist only in the unstable region in which the absolute vorticity changes sign relative to that of the remainder of the hemisphere in which the instability exists. It is immediately apparent that departures from conservative motion are not required to bring about the instability, unlike the initially stable extra-tropical case, since potential vorticity is a conserved quantity, and cross-equatorial motion, instead of non-conservative motion, generates an unstable state. (It will be noted, however, that nonconservative effects in the far field, such as high-latitude diabatic heating and cooling, may ultimately be responsible for the cross-equatorial flow.)

Kinematically this equatorial inertial instability is a member of the class of "parcel instabilities." In the unstable region, a parcel travelling to the north is deflected to the west, and then to the north, and so on, resulting in unstable growth of the parcel displacement instead of a stable inertial oscillation. Constraints of mass continuity create vertical divergence and convergence near the edges of the unstable region, resulting in overturning and thus adiabatic temperature perturbations. The latter generate hydrostatic pressure perturbations which act to partially offset the meridional motions, as shown in Fig. 1.

In terms of equatorial wave theory, the inertial or centrifugal instability belongs to the "gravitational" class. Another type of wave also belonging to the gravitational class is the equatorial Kelvin wave. It was recently demonstrated that the Kelvin wave is unstable in linear cross-equatorial shear (Boyd and Christidis, 1982). Unlike the symmetric inertial instability but more akin to the familiar shear instabilities, the Kelvin-wave instability contains a "critical latitude," or critical surface, at which point the Doppler-shifted real frequency component vanishes. Judging by the appearance of the unstable eigenfunction and mean flow acceleration (see Boyd, 1982), this critical lati-

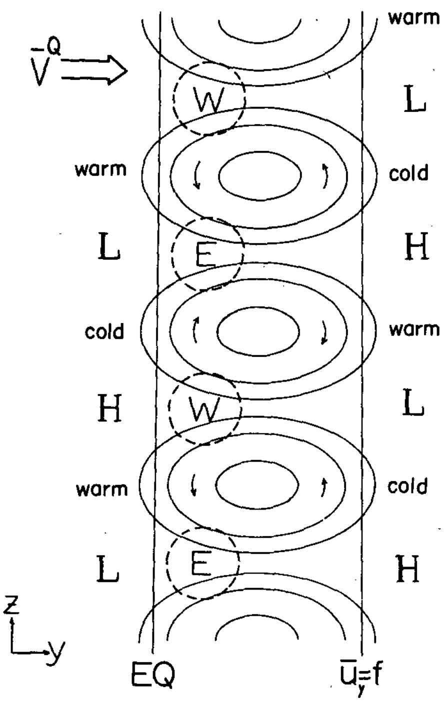

FIG. 1. Vertical structure of the symmetric instability, from Dunkerton (1981).

tude plays a crucial role in the Kelvin-wave instability. Furthermore, the qualitative behavior of the growth rate as a function of shear strength is suggestive of a possible overreflection interpretation. However, such an interpretation must await further investigation of the Kelvin-wave instability.

The purpose of this note is not to further explore this interpretation, but to present a numerical investigation of zonally *nonsymmetric* equatorial inertial instability at finite zonal wavenumber. In the earlier paper (Dunkerton, 1981), the author confined attention to the zonally symmetric modes, which are the only known analytic solutions without recourse to perturbation methods. Zonal nonsymmetry was excluded because of the lack of known analytic solutions, and not because of any prejudged irrelevance. As further light dawned on this subject, however, it became clear that the nonsymmetric modes would also need to be considered via numerical methods.[1] The reason is that in some situations the nonsymmetric modes of instability are preferred over their symmetric counterparts. The qualifying clause "in some situations" is necessary because of the role of scale-dependent dissipation and the discreteness of zonal wavenumbers on the spherical earth, of which more will be said later.

In view of the contiguity between the Kelvin and inertial instabilities, following Boyd and Christidis (1982), I will label the instability as the Kelvin-inertial (KI) instability and mention two implications of this fact before continuing the discussion. First, Kelvin-wave behavior exists at the lower end of the growth rate axis, and consequently Kelvin-wave instability is not expected to be observed in the real world unless factors other than growth rate alone are important in the selection of instability. Second, the distinction between shear and parcel instability is no longer clear, since both mechanisms are operative in the KI instability in different regions of parameter space. These results suggest that the relationships between shear and parcel instabilities need to be further explored, not only in the present case, but perhaps also in other instabilities as well.

In the next section, some background is given for the Kelvin and symmetric inertial instabilities. In Section 3 the numerical results for nonsymmetric instability are presented. A crucial result is the existence of a short wave cutoff for equatorial waves in linear shear on the unbounded beta-plane, and thereby the development of marginal stability criteria in the presence of second-order diffusion. Zonal nonsymmetry is found to reduce the marginally stable shear by as much as 26% from that of the symmetric case investigated by Dunkerton (1981). Again, the qualifier "as much as" is necessary in view of the discreteness of zonal wavenumbers on the spherical earth.

2. Background

In this section we briefly review the marginal stability criteria for symmetric instability on the equatorial beta-plane, the instability of the Kelvin wave in linear cross-equatorial shear, and the contiguity between the Kelvin and inertial instabilities.

a. Symmetric inertial instability

The dimensional "dispersion relation" for symmetric instability on the equatorial beta-plane with constant shear, stratification, and density is

$$\omega^2 = N\beta/|m| - \gamma^2/4, \qquad (2.1)$$

where γ is the shear $\bar{u}_y$; ω, N, β, and m are frequency, static stability, planetary vorticity gradient, and vertical wavenumber, respectively. Eq. (2.1) indicates that in the absence of scale-dependent dissipation, fastest growth occurs at infinite m at which point $\omega_i = \frac{1}{2}\gamma$, which is equal to the Coriolis parameter in the center of the unstable region bounded below by the equator (for positive shear) and above by the point where $\gamma = \beta y$. When a second-order diffusion is included in the equations, with Prandtl number equal to unity, a marginally stable shear is found to be

$$|\gamma_c| = 2\sqrt{5}\nu^{1/5}(N\beta/4)^{2/5}, \qquad (2.2)$$

[1] I am indebted to Professor John Boyd for originally bringing to my attention the results of the "gamma-plane" approximation indicating the increase in growth rate for infinitesimally small zonal wavenumbers off the symmetric axis.

where ν is the diffusion coefficient (Dunkerton, 1981). Maximum growth now occurs at finite m:

$$|m_c| = \left(\frac{N\beta}{4\nu^2}\right)^{1/5}, \tag{2.3}$$

which together with (2.2) defines the onset of symmetric instability in this case.

The vertical structure of the symmetric instability is shown in Fig. 1. The instability is clearly centrifugal in the sense that Coriolis forces are primarily responsible for the instability without reference to thermal or buoyancy effects. In this case, the growth of the disturbance, due to the correlation of northward and westward perturbation velocity components, is being exactly balanced by diffusion. The entire disturbance is symmetric about the "shifted equator" at the center of the unstable region.

b. Kelvin-wave instability

The instability of the Kelvin wave in linear cross-equatorial shear was discovered by Boyd (1982) and discussed in considerably more detail in a note by Boyd and Christidis (1982). Those authors used a nondimensional notation related to the dimensional variables as follows:

$$k^* \equiv \epsilon_H^{-1/4} s \equiv \epsilon_H^{-1/4} ka, \tag{2.4a}$$

$$\omega^* \equiv \epsilon_H^{1/4} \sigma \equiv \epsilon_H^{1/4}(\omega/2\Omega), \tag{2.4b}$$

$$S^* \equiv \epsilon_H^{1/4} S \equiv \epsilon_H^{1/4}(\gamma/2\Omega), \tag{2.4c}$$

$$\epsilon_H \equiv (2\Omega a)^2 \epsilon, \tag{2.4d}$$

where k is dimensional zonal wavenumber, a is the radius of the earth, $\Omega = 7.29 \times 10^{-5}\ \mathrm{s}^{-1}$, and ϵ is the eigenvalue of the separable "shallow water" equations, related to the vertical wavenumber as

$$\epsilon \equiv \frac{m^2}{N^2}. \tag{2.5}$$

The Kelvin-wave growth rate was determined by curve-fitting to be given by the approximate formula

$$\lim_{k^*\to 0} \omega_i^* = (13.56k^*) \exp(-5.34S^{*-1}), \tag{2.6}$$

in the range $0.4 < S^* < 1.15$. Below $S^* = 0.4$ growth rates were too small to determine accurately. As S^* is increased above 1.15, a maximum is reached at $S^* = 1.84$. Thereafter, the growth rate drops rapidly to zero just ahead of $S^* = 2$. Comparison of (2.4) to (2.1) indicates that the latter point is the mathematical neutral point for the symmetric instability. Above this point the growth rate increases precipitously like $\frac{1}{2}(S^{*2} - 4)^{1/2}$ and is much larger than the maximum Kelvin wave growth rate found below $S^* = 2$.

c. Contiguity of the Kelvin and inertial instabilities

From the foregoing paragraph there appears to be a clear distinction between the Kelvin and inertial instabilities in the limit of vanishing zonal wavenumber. This distinction evidently reflects the different physical mechanisms underlying the two types of instability. However, one may raise the issue of relevance, noting that (2.6) implies a vanishingly small growth rate for the Kelvin wave instability. On the other hand, Eq. (2.6) implies that larger zonal wavenumbers increase the growth rate. Using the "gamma-plane" approximation, a perturbation expansion in k^*, it has been shown (in the first version of Boyd and Christidis, 1982) that a similar increase in growth rate with increasing k^* is observed for the inertial instability in the range $2 < S^* < 3$. Unfortunately, however, the numerical formula (2.6) and the analytic result (2.1) are not valid at finite k^*, nor is the gamma-plane approximation.

This note will provide a numerical investigation of the inertial instability at finite zonal wavenumber. It will be shown that a short-wave cutoff

$$|k\gamma| = \beta, \quad (k^*S^* = 1) \tag{2.7}$$

implies the existence of a maximum growth rate for the inertial instability below this cutoff value. Boyd and Christidis (1982) demonstrated that the Kelvin and inertial instabilities represent one and the same mode. Importantly, this result implies that if marginal stability criteria can be established for the inertial instability at finite zonal wavenumber, the existence of the Kelvin-wave limit of the instability will have no effect on these criteria, since this limit implies a vanishingly small growth rate. In other words, if the net growth rate alone is regarded as the quantity which defines marginal stability criteria, the Kelvin-wave behavior in a certain region of the parameter space is irrelevant to these criteria.

These remarks should not convey the impression that the Kelvin-wave instability is itself irrelevant, since other factors in addition to the net growth rate, such as the mechanisms of excitation, may be relevant to the appearance of hydrodynamic instabilities (e.g., Dickinson and Clare, 1973).

In the next section, a Hermite spectral method is employed to determine growth rates for the KI instability at finite zonal wavenumber. This method was found to be suitable only in the "inertial" limit of the instability, because the critical latitude singularity cannot be well-resolved by the spectral model. However, it was found that with second-order diffusion the marginal stability criteria could be determined numerically without reference to the distinctly "Kelvin" behavior of the KI instability at small growth rate. It was then determined that the marginally stable shear is approximately 26% less than the symmetric value (2.2).

Boyd and Christidis (1982) also found a secondary instability in this problem which, as a function of increasing nondimensional shear, begins as a stable eastward-propagating inertia–gravity wave and is transformed into a very weak Kelvin-type instability for $S^* > 2$. In view of the weak growth exhibited by this mode, it will not be further discussed here.

3. Instability at finite zonal wavenumber

Equatorial waves and instabilities are governed by the geopotential equation

$$\frac{d}{dy}\left(\frac{\phi_y}{\Delta}\right) - \frac{\phi}{\Delta}\left[k^2 + \frac{k\beta}{\hat{\omega}\Delta}(y\Delta_y - \Delta)\right] = \epsilon\phi, \quad (3.1)$$

where in linear shear

$$\hat{\omega} = \omega - k\gamma y, \quad (3.2a)$$

$$\Delta = \beta y(\beta y - \gamma) - \hat{\omega}^2. \quad (3.2b)$$

a. Hermite spectral model

To solve (3.1), the Hermite spectral series is substituted

$$\phi(y) = \sum_{n=1}^{N} \phi_{n-1} H_{n-1}(\xi) \exp(-\xi^2/2), \quad (3.3)$$

where

$$\xi \equiv (y - \gamma/2\beta)/y_0. \quad (3.4)$$

The shifted latitudinal coordinate is used because shifted Hermite functions are exact solutions to the symmetric problem with linear shear (Dunkerton, 1981). This spectral method is suitable if the critical latitude singularity is unimportant to the instability, as is the case in the strong centrifugal instabilities. The Kelvin–wave limit of the instability must, however, be explored with complex integration, and is not discussed in detail here. Except at very small growth rates, we find rapid convergence in the series (2.3) even when $k \neq 0$.

The substitution (3.3) yields a matrix eigenproblem which is solved by truncation (in the present case $N = 40$). The latitudinal scale is set near the scale of the symmetric eigenfunction. For instability, the procedure is to specify the growth rate as some fraction of $\frac{1}{2}\gamma$, and then iterate the *real* frequency component to yield a real eigenvalue. The latter is required to satisfy the unbounded vertical structure equation which is assumed *a priori* in this problem.

b. Short-wave cutoff

For exponential decay at large $|y|$, Eq. (3.1) requires that Δ be an upward parabola at large $|y|$, which in turn requires that for waves and instabilities on the unbounded equatorial beta-plane,

$$|k\gamma| < \beta. \quad (3.5)$$

Since it has already been established by Boyd and Christidis (1982) that an increase in growth rate is possible as the zonal wavenumber is initially increased above zero, a maximum growth rate at some zonal wavenumber between the symmetric value and the short-wave cutoff is also possible.

One should not overlook the discreteness of zonal wavenumbers on the spherical earth. Should the growth rate maximum occur, say, as $s = \frac{1}{3}$, with smaller growth at $s = 1$ than at $s = 0$, then the instability will remain symmetric. These considerations will enter the discussion of marginal stability below.

c. Numerical results

I will begin by citing a specific example, before allowing it to be generalized to all values of shear in the next subsection. In this example, shown in Fig. 2, $\gamma = 10^{-5}\ s^{-1}$, a value typical of the order of magnitude of cross-equatorial shears found in the mesosphere at the solstices (although a factor of three or more smaller than the maximum climatological shears at this time). Fig. 2a displays the growth rate as a fraction of its maximum, $\frac{1}{2}$. The symmetric instability corresponds to $s = 0$, while the vertical dashed line beyond $s = 14$ denotes the short-wave cutoff. The slanted dashed line approximately traces out the maximum growth rate as a function of zonal wavenumber. Of course, in the *inviscid* case, assuming growth rate alone determines the appearance of the instability, symmetric instability is clearly preferred, having the maximum rate of growth at infinite eigenvalue, or vanishing vertical scale. However, if some damping process, such as a scale dependent dissipation, tends to inhibit the very short vertical scales, then there exists a possibility that the instability will be nonsymmetric. In the next subsection, more will be said regarding marginal stability criteria for the nonsymmetric instability.

Fig. 2b shows the ratio of real to imaginary phase speed for some of the contours of Fig. 2a. The KI instability exhibits positive phase speeds except at small growth rates and small zonal wavenumber.

The latter region evidently corresponds to the "Kelvin" region of the instability. Referring back to Fig. 2a, there would be a second ridge of maximum growth rate (not shown), this time as a function of eigenvalue, in the lower left hand corner below $s = 2$ and $\epsilon = 0.8$. This second ridge corresponds to the peak in imaginary phase speed found by Boyd and Christidis (1982) mentioned above. Because the critical latitude is important here, the spectral model was not used to plot additional contours much below 0.1. In the present example, however, this second ridge would intersect the symmetric axis at $\epsilon = 0.605$ (with the growth rate itself going to zero as s approaches 0).

Fig. 2a indicates that the infinitely steep increase in growth rate above the neutral point $(s, \epsilon) = (0, 0.84)$ extends into the finite s domain as a precipitous cliff slanting downward in the (s, ϵ)-plane as s is increased. At larger zonal wavenumbers there is no longer any such cliff. Except for the distinctly "Kelvin" wave behavior in the lower left hand corner of Fig. 2a, the instability is primarily inertial, or centrifugal, in nature. This will be evident when the structure of the nonsymmetric instability is further discussed in Section 3e below.

d. Marginal stability criteria

The nondimensionalization (2.4) has the effect of parametric reduction by removal of the eigenvalue from the shallow water equations and hence from the geopotential equation (3.1). The information in Fig. 2a can therefore be used to construct a nondimensional plot

$$\omega^* = \omega^*(k^*, S^*), \qquad (3.6)$$

with k^* and S^* on the horizontal and vertical axis, respectively. The short-wave cutoff is now a hyperbola $k^*S^* = 1$, but above the neutral point the growth rate contours continue to bend down as a function of increasing k^* as long as $S^* \leqslant 3$ (Boyd and Christidis, 1982, original version).

More importantly, the marginally stable shear can be derived easily from the numerical calculations. Returning for the moment to the dimensional Fig. 2a, it is possible to calculate at each and every point in the figure a "stabilizing viscosity" which results in *neutrality*, i.e.,

$$\nu m^2 = \nu \epsilon N^2 \equiv \omega_i \qquad (3.7)$$

(although it is recognized that the viscous problem is inseparable in y, z, and more investigation is needed). The preferred mode of instability then corresponds to the point in the (s, ϵ)-plane which maximizes the stabilizing viscosity, since at all other points the same viscosity would result in decay, not neutrality. This can be done in any specific case, such as Fig. 2a, but more importantly the procedure also may be applied to the nondimensional plot (3.6), which generalizes the result to any dimensional shear. After a little manipulation, it is apparent that maximizing the stabilizing viscosity also maximizes the quantity

$$\frac{\omega_i^*}{S^{*5}} \qquad (3.8)$$

for a given dimensional shear (and N, β held constant). Now let us put the result in reverse: If, for a given dimensional viscosity, we can find the point requiring the *least* dimensional shear for neutrality, then we have determined the onset of instability in the presence of second-order diffusion. But this is the point that minimizes the inverse of the same quantity in (3.8). Inspection of the numerical calculations suggests approximately that

$$|\gamma_c| = (0.74)2^{1/5}\sqrt{5}\nu^{1/5}(N\beta)^{2/5}. \qquad (3.9)$$

In Fig. 2a, this point is found near the 0.1 contour

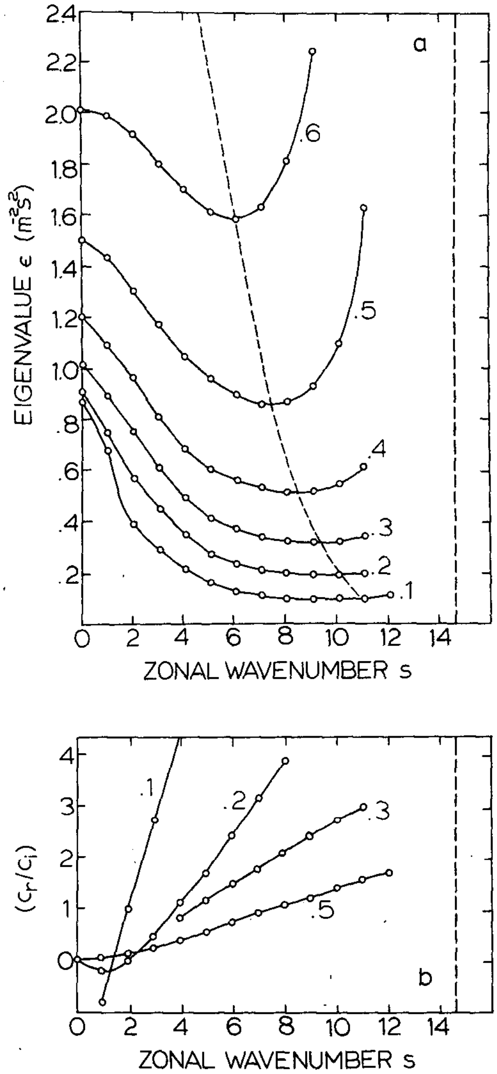

FIG. 2. Eigenvalues and real phase speeds for the centrifugal instability as a function of zonal wavenumber for the case discussed in the text. Contours are labelled with the ratio of ω_i to its maximum, $\frac{1}{2}\gamma$.

and in the vicinity of $s = 11$. For this shear, the viscosity required to stabilize the flow is about 4½ times that which is sufficient to stabilize the flow with respect to *symmetric* inertial instability. The vertical wavelength is on the order of 4 times larger than that of the symmetric viscous neutral mode.

The presence of very large viscosities requires caution, for it is then possible that all nonzero wavenumbers might be excluded by the short-wave cutoff. This is why the formula (3.9) is to be regarded as a lower bound on the critical shear.

e. Structure of the nonsymmetric instability

It is possible to show how the various wave fields interact in a nonsymmetric inertial instability. In gen-

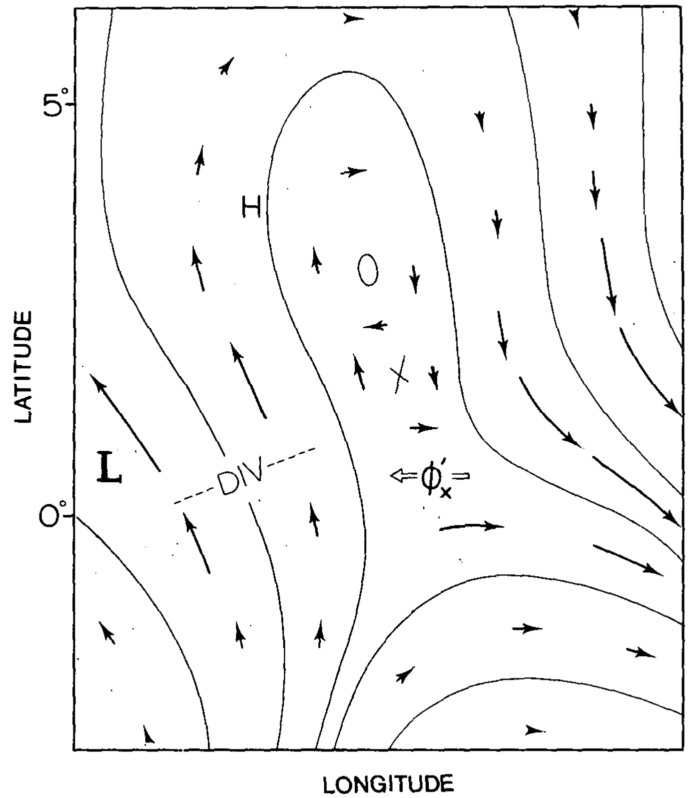

FIG. 3. Horizontal structure of the nonsymmetric instability with $\gamma = 10^{-5}$ s^{-1}, $s = 7$ and $\omega_i = \frac{1}{4}\gamma$. Contours are tangential to the instantaneous velocity field (not to be confused with parcel trajectories). Length of arrows (excluding arrowheads) indicates the velocity magnitude. The longitudinal (horizontal) axis is compressed by roughly a factor of 3. The symbols L and H indicate low and high pressure, and DIV denotes the region of large horizontal divergence. The figure displays a ½-zonal wavelength.

eral, at large growth rates the instability looks like its symmetric counterpart, whose vertical structure is reproduced here in Fig. 1. However, the introduction of the zonal dependence suggests that the longitudinal divergence and longitudinal pressure gradient force are brought into play in the instability. An explanation of their effect might begin by noting that a horizontal divergence is implied by u'_x just north of the equator. Because this divergence implies the formation of low pressure by the continuity and hydrostatic relations, there is an implied positive phase speed of the disturbance, noting that the region of low pressure is originally associated with negative u' to the west of the region of divergence u'_x. The longitudinal pressure gradient force appears to accelerate u' in a westward sense in this region, consistent with phase speeds of positive sign. Because u'_x is strongest south of the midpoint $\gamma = 2\beta y$, there is also an implied asymmetry in the geopotential about the midpoint, being stronger to the south. This discussion is found to be consistent with the structure of the eigenfunction when $\omega_i = \frac{1}{4}\gamma$ and $s = 7$, as shown in Fig. 3. The momentum flux (not shown) is quantitatively similar to that of the symmetric instability (Fig. 4 of Dunkerton, 1981) and is negative except for a small positive component north of the instability boundary $\gamma = \beta y$.

There may exist an analogy, albeit a very crude one, between the effects of nonsymmetry and thermal dissipation. As noted in the earlier papers, the symmetric instability is aided by thermal damping insofar as the hydrostatic pressure perturbations oppose the meridional motions (Fig. 1). In the nonsymmetric instability, parcel motions are altered so as to take advantage of the pressure gradient force to the extent that this is possible. To grow efficiently, however, the instability must maintain a strong negative correlation $\overline{u'v'}$. Certainly this is why the Kelvin-wave limit is weak, in view of the smallness of v' in the neutral Kelvin wave.

4. Conclusions

In addition to the questions regarding the inertial stability of the equatorial middle atmosphere (Dunkerton, 1981) there are two new interesting developments: The Kelvin wave is unstable in a linear cross-equatorial shear (Boyd and Christidis, 1982) while at finite zonal wavenumber both the Kelvin and inertial instabilities reveal themselves as being one and the same mode. By implication, there exists a possibility of nonsymmetric instability on the equatorial beta-plane. Significantly, this result does not require the Prandtl number to be different from unity, as was the case in the baroclinic inertial instability problem addressed by Busse and Chen (1981). The effect of Prandtl number variations in equatorial symmetric instability was recently discussed by Dunkerton (1982).

These new analytical results point to some relevant questions in the equatorial middle atmosphere:

1) Are realistic equatorial middle atmosphere states, with realistic models of dissipation, unstable to either Kelvin or centrifugal type disturbances?

2) Is the unstable growth dictated strictly by the maximum growth rate, or is there a dependence on the amount of energy initially available at each zonal wavenumber?

3) Do significant wave, mean-flow interactions result from either instability, and is the stratopause semiannual oscillation affected insofar as it is partly due to cross-equatorial advection?

The first question would require consideration of the acceleration in the radiative damping rate found by Fels (1982), and would also be intimately related to the occurrence, or otherwise, of breaking gravity waves in the equatorial mesosphere (Lindzen, 1981). The second question is particularly important in the middle atmosphere in view of the dominance of zonal wavenumbers 0–3 in the basic state.

Acknowledgments. Helpful discussions with John Boyd and K. K. Tung are gratefully acknowledged, together with a very constructive review by Duane Stevens. This research was performed at the National Center for Atmospheric Research, which is sponsored by the National Science Foundation.

REFERENCES

Boyd, J. P., 1982: The influence of meridional shear on planetary waves, Part II: Critical latitudes. *J. Atmos. Sci.*, **39**, 770–790.

——, Z. D. Christidis, 1982: Low wavenumber instability on the equatorial beta-plane. *Geophys. Res. Lett.*, **9**, 769–772.

Busse, F. H., and W. L. Chen, 1981: On the (nearly) symmetric instability. *J. Atmos. Sci.*, **38**, 877–880.

Dickinson, R. E., and F. J. Clare, 1973: Numerical study of the unstable modes of a hyperbolic-tangent barotropic shear flow. *J. Atmos. Sci.*, **30**, 1035–1049.

Dunkerton, T. J., 1981: On the inertial stability of the equatorial middle atmosphere. *J. Atmos. Sci.*, **38**, 2354–2364.

——, 1982: The double-diffusive modes of symmetric instability on an equatorial beta-plane. *J. Atmos. Sci.*, **39**, 1653–1657.

Fels, S. B., 1982: A parameterization of scale-dependent radiative damping rates in the middle atmosphere. *J. Atmos. Sci.*, **39**, 1141–1152.

Lindzen, R. S., 1981: Turbulence and stress due to gravity wave and tidal breakdown. *J. Geophys. Res.*, **86C**, 9707–9714.

——, and K. K. Tung, 1978: Wave overreflection and shear instability. *J. Atmos. Sci.*, **35**, 1626–1632.